



ISTITUTO NAZIONALE DI GEOFISICA E VULCANOLOGIA

**ACCEPTED ON ANNALS OF GEOPHYSICS, 63, 2020; doi:
10.4401/ag-8327**

**“An integrated geodetic and InSAR technique for the
monitoring and detection of active faulting in
southwestern Sicily,”**

**Giovanni Barreca^c, Valentina Bruno^a, Gino Dardanelli^b, Francesco
Guglielmino^a, Mauro Lo Brutto^b, Mario Mattia^{a*}, Claudia Pipitone^b,
Massimo Rossi^a**

^a Istituto Nazionale di Geofisica e Vulcanologia, Osservatorio Etneo, Piazza Roma 2,
95123 Catania, Italy

^b Università degli Studi di Palermo, Dipartimento di Ingegneria, Palermo, Italy

^c Università degli Studi di Catania, Dipartimento di Scienze Geologiche, Biologiche ed
Ambientali, Catania, Italy

1 **An integrated geodetic and InSAR technique for the monitoring and detection of**
2 **active faulting in southwestern Sicily**

3 G. Barreca^c, V. Bruno^a, G. Dardanelli^a, F. Guglielmino^a, M. Lo Brutto^b, M. Mattia^{a*}, C.
4 Pipitone^a and M. Rossi^a

5 ^a *Istituto Nazionale di Geofisica e Vulcanologia, Osservatorio Etneo, Piazza Roma 2, 95123 Catania, Italy*

6 ^b *Università degli Studi di Palermo, Dipartimento di Ingegneria, Palermo, Italy*

7 ^c *Università degli Studi di Catania, Dipartimento di Scienze Geologiche, Biologiche ed Ambientali, Catania,*
8 *Italy*

9

10 **Abstract**

11 We present the results of the analysis of GNSS (Global Navigation Satellite System) and
12 InSAR (Interferometric synthetic-aperture radar) data collected in the frame of a project
13 financed by the “Struttura Terremoti” of INGV (Istituto Nazionale di Geofisica e
14 Vulcanologia). Combined investigations pointed out for potential seismogenic sources of
15 destructive earthquakes recorded in southwestern Sicily, including the 1968 Belice
16 earthquake sequence and those supposed to have destroyed the Greek city of Selinunte
17 which, according to geoarcheological data, experienced two earthquakes in historical
18 times. Our approach is aimed to evaluate the current deformation rate in SW Sicily and to
19 improve the knowledge about the seismic potential of this area. The geodetic data proposed
20 in this paper show that the Campobello di Mazara–Castelvetrano alignment (CCA) is
21 currently deforming with a vertical and horizontal displacements of 2 mm/yr and 0.5
22 mm/yr respectively, according to the tectonic setting of the area.

23

24 *Keywords:* Belice earthquake, GNSS data, InSar data, Geodesy

25

26 * Corresponding author. Tel.: +39 095 7165800; E-mail address: mario.mattia@ingv.it
27 (M.Mattia)

28

29

30

31

32 **1. Introduction**

33 Although the investigated area has been occasionally hit by strong earthquakes both in
34 recent and historical time (e.g. Belice, 1968 and Selinunte events CPTI11, Rovida et al.,
35 2011, Guidoboni et al., 2002; Bottari et al., 2009), data about the pattern of active
36 deformation are scarce and/or poorly constrained. This is mainly related to the low rate of
37 deformation affecting the southwestern Sicily, which did not allow to the development of
38 prominent morpho-structural expressions of possible active tectonic structures. Even if
39 both historical and instrumental records reveal that the seismicity of southwestern Sicily is
40 characterized by sparse, low-moderate magnitude earthquakes (ISIDE database;
41 <http://iside.rm.ingv.it/iside/standard/index.jsp>; see also Rigano et al., 1999; Rovida et al.,
42 2011), the occurrence of strong earthquakes in the past suggest instead the investigated
43 area as having a high seismic potential. However, exhaustive information on the location,
44 kinematics and dimensions of the active tectonic structures responsible for large
45 earthquakes in the area are still lacking and/or their rate of deformation is not fully
46 understood. This uncertainty reflects in official databases, such as DISS, where the
47 proposals on seismogenic sources capable of generating earthquakes with $M > 5.5$ are
48 preliminary and based on the few data available in the literature (Diss Working Group,
49 2010). Geodetic observations, very useful to clarify the nature of deformation on a regional
50 scale (Ferranti et al., 2008; Devoti et al., 2011; Palano et al., 2012), have also been able to
51 provide constraints on the position and nature of the active structures in SW sector of
52 Sicily (Barreca et al., 2014).

53 With the aim to investigate the dynamics of active tectonic structures occurring in SW
54 Sicily and to understand how stress is dissipated through time, a new set of GNSS data has
55 been collected by using both permanent and episodically surveyed stations.. Further, we
56 performed the SENTINEL 1A-1B DInSAR analysis covering the 2015-2019 time span to
57 investigate the short-term dynamics of the active faults deforming the investigated area.
58 More specifically, we focused on the sector in-between Campobello and Castelvetro
59 (Fig.1) localities, where an active fault segment was already identified by previous authors
60 (see Barreca et al. 2014).

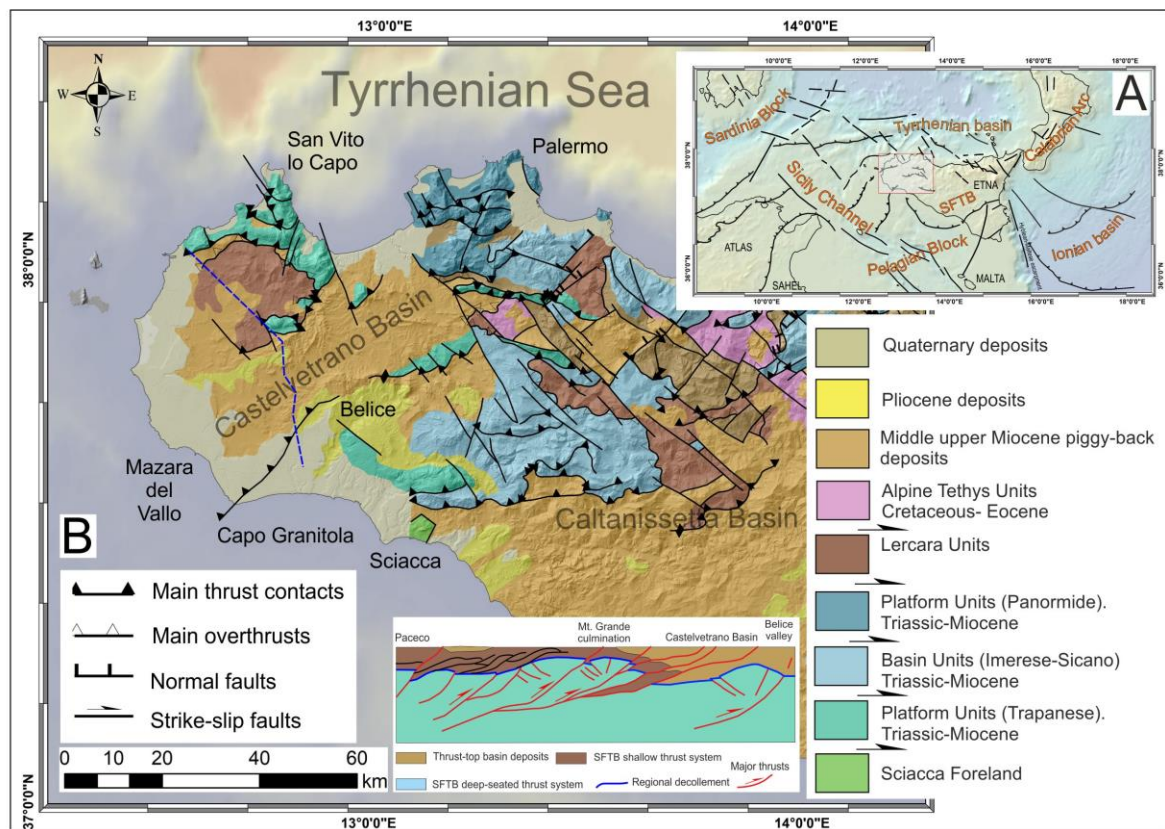
61 Results, lastly framed in the larger geodynamic context of Sicily, confirm the meaningful
62 deformation rate across the Campobello di Mazara–Castelvetro active structure and
63 permits new insights for the evaluation of its seismic potential in the light of the
64 earthquakes occurred in the past.

65 **2. Background**

66 *2.1 Geological setting*

67 The investigated area in SW Sicily represents the westernmost part of the Sicilian Fold and
68 Thrust Belt (hereafter, SFTB, Fig. 1A), a south-verging contractional belt segment of the
69 wider Apennine-Maghrebian orogenic system, the suture zone between the colliding
70 Africa and European plates (Dewey et al., 1989; Ben Avraham et al., 1990). The SFTB is
71 the result of the Neogene-Quaternary tectonic processes during which a pre-orogenic
72 configuration (formed at that time by both platform and open-shelf rock series, i.e. the
73 African continental paleo-margin) has been progressively shortened to form a wide
74 thrusting system. The westernmost segment of the SFTB (i.e. the studied area), consists of
75 NE-SW trending structural domains composed of several, thrust-bounded, foreland-
76 verging tectonic blocks (Fig. 1B) at present interposed between two extensional domains,

77 the Tyrrhenian Basin to the north and the stretched Sicily channel region to the south (Fig.
 78 1A). Deep seismic explorations in the area (Catalano et al 1989, 2000), revealed the
 79 structural architecture of SW Sicily as formed by two overlapping thrust wedges separated
 80 by a regional decollement. In this duplex-shaped deformation context, the upper structural
 81 layer consists of a thin (1-3Km thick), small-wavelength fold and thrust system while the
 82 lower



83
 84 **Figure 1.** a) Tectonic model of the Central Mediterranean region where SFTB occur. Lines represent the
 85 main faults. Lines with triangles represent the main contractional tectonic features. (b) Geological sketch map
 86 of central-western Sicily (from Finetti et al., 2005, modified) and schematic, not-in-scale cross-section
 87 the investigated area (From Catalano et al., 1989 modified) showing the outcropping tectonic units and
 88 contacts (mostly thrust and strike-slip faults) and their architecture at depth, respectively..

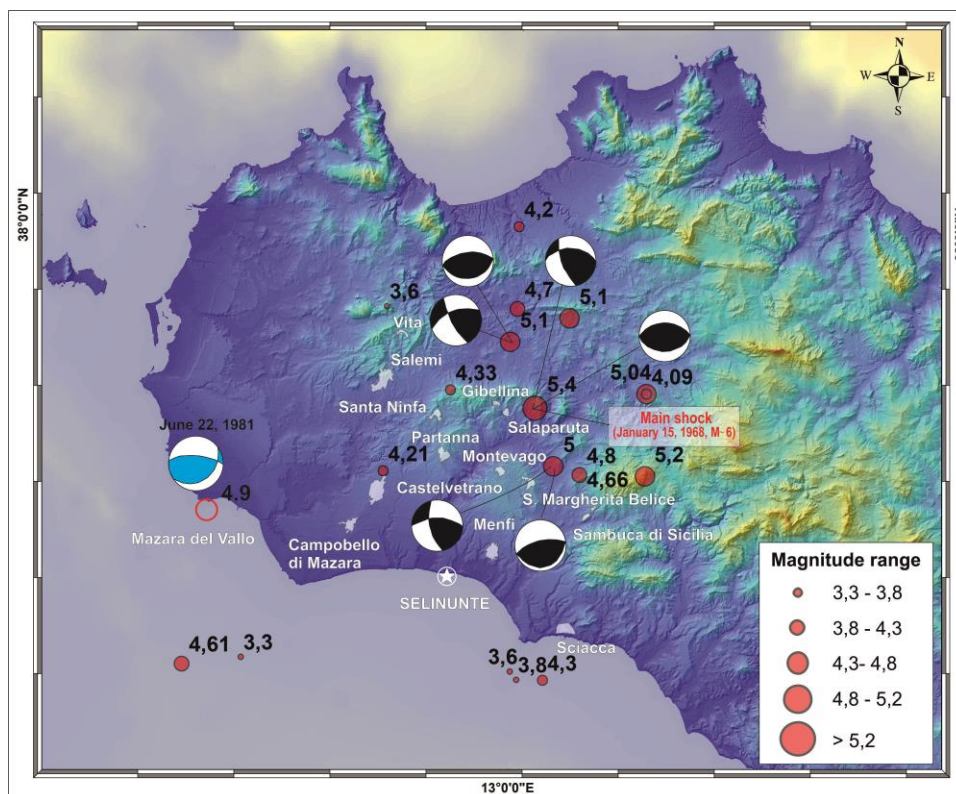
89 is given by a thicker (~10 km) thrust stack (Catalano et al., 2000) resulting by the
 90 deepening of thrust contacts in response to the Late Miocene-Early Pliocene collisional
 91 processes (Bello et al., 2000, Catalano et al., 2000; Avellone et al., 2010; Barreca et al.,

92 2010; Barreca and Maesano, 2012). The propagation of the younger, deep-seated thrusting
93 re-deformed the previously stacked tectonic units (e.g. the overlain thrust wedge – middle
94 Miocene) and was accompanied by the development of large marine basins at the footwall
95 of major contractional structures. This later process and the resulting tectonic structures are
96 considered to be still active and have been retained to be responsible for the nucleation of
97 large earthquakes in the area (e.g. the 1968 Belice seismic crisis, see Monaco et al., 1996,
98 Lavecchia et al., 2007; Barreca et al., 2014). Accordingly, the seismotectonic processes
99 that involve this region appear to be related to ongoing compressional activity along deep-
100 seated, high-angle thrust contacts that, at a shallower crustal level, display flat-ramps
101 geometries of deformation. Clues for a recent tectonic activity came only from slightly
102 folded Holocene lacustrine deposits in the frontal part of the tectonic stack (Monaco et al.,
103 1996 and reference therein) and from faulted archaeological remains (Barreca et al., 2014).
104 However, the clayey lithology occurring in the area and the low rate of deformation make
105 difficult the identification of surface expression of active faults, being the latter rapidly
106 modelled by erosive processes.

107 *2.2 Seismotectonic*

108 Apart from the Palermo (1726, 1734, 1940, 2002) and Belice (1968) earthquakes, historical
109 and instrumental records (Pondrelli et al., 2006; Guidoboni et al., 1994) reveals that the
110 seismicity of western Sicily is characterised by only a few moderate magnitude
111 earthquakes with epicentres spread from the Tyrrhenian coast to the Sicily Channel. In
112 fact, before the 1968 Belice seismic sequence, the most significant seismic event occurred
113 in the area after the Roman colonization, the westernmost segment of the SFTB was
114 considered a rather seismically quiescent region. Nevertheless, archaeological evidences
115 analyzed in the last decade (e.g. Guidoboni et al., 2002; Bottari et al., 2009) suggest also
116 the occurrence in the area of two ancient and strong earthquakes (between 370 and 300

117 B.C. and between 300 and 600 A.D.) that destroyed the Greek colony of Selinunte in the
 118 South-west coast of Sicily (see Fig. 2 for location). The 1968 seismic swarm nucleated at
 119 shallow to middle crustal domain with focal depths ranging from 1 to 39 km (Anderson
 120 and Jackson,1987) while epicenters (Fig. 2) distributed over a large part of south-western
 121 Sicily (De Panfilis and Marcelli 1968, Marcelli and Pannocchia, 1971; Bottari, 1973,
 122 Anderson and Jackson,1987) including the Tyrrhenian coast (to the north) and the Sciacca
 123 off-shore (to the south). Most of seismic events localized within the NE-SW trending
 124 Castelvetroano structural depression (Fig. 1B) where a number of events clustered around
 125 the Belice River valley with a main gathering in the nearby of Poggioreale, Salaparuta and
 126 Gibellina villages (Fig. 2).



127
 128 **Figure 2.** Seismic events distribution, magnitude and focal solution of the 1968 earthquake sequence (from
 129 Anderson and Jackson, 1987). Focal solutions show either right-lateral strike-slip or thrust focal mechanisms.
 130 Light blue focal mechanism is that of the 1981 Mazara earthquake (from Pondrelli et al.,2006).

131 According to the focal solutions proposed in the literature (mainly coming from the Belice
132 1968 seismic sequence, see Fig. 2), the seismotectonic processes in the area are governed
133 by a nearly N–S trending P-axis, compatible with a right-lateral component of motion
134 along NNW-striking planes or, alternatively, with thrusting mechanisms along ENE-
135 trending planes (Anderson and Jackson, 1987). An almost pure reverse mechanism with a
136 nearly N–S trending P-axis is also provided by the Mazara 1981 earthquake ($M_w=4.9$),
137 located about 30 km to the west of the Belice area (Pondrelli et al., 2006; Lavecchia et al.,
138 2007, see Fig. 2 for location).

139 *2.3 The 1968 Belice seismic sequence*

140 At 2.01.04 (GMT) of January 15, 1968, a wide area of western Sicily was hit by a strong
141 ($M \sim 6$, De Panfilis and Marcelli 1968; Anderson and Jackson, 1987) earthquake, the main
142 shock of a high frequency seismic swarm (more than 300 events) that shaken the region for
143 about a month later. The disastrous event, the strongest seismic event recorded in Western
144 Sicily in historical time, was preceded by a series of minor events (on January 14 with $4.7 <$
145 $M < 4.9$) and followed by several aftershocks, among these the events of 16 and 25 January
146 reached the magnitude of 5.7 (De Panfilis and Marcelli 1968; Bottari, 1973; Anderson and
147 Jackson, 1987). The seismic event caused about 370 deaths and severe damaging on
148 fourteen villages facing the Belice river valley. Four of these (Gibellina, Poggioreale,
149 Salaparuta and Montevago) were completely destroyed. Ground effects related to 1968
150 earthquakes were generally scarce and occurred mainly at the northern limb of Belice
151 syncline and consisted of moderate landslides, mud upraise along fractures and fluids
152 escape (Michetti et al., 1995; Bosi et al., 1973). Sand blows and fissures related to
153 liquefactions phenomena was observed along the Belice alluvial river plain (Haas and
154 Ayre, 1969)

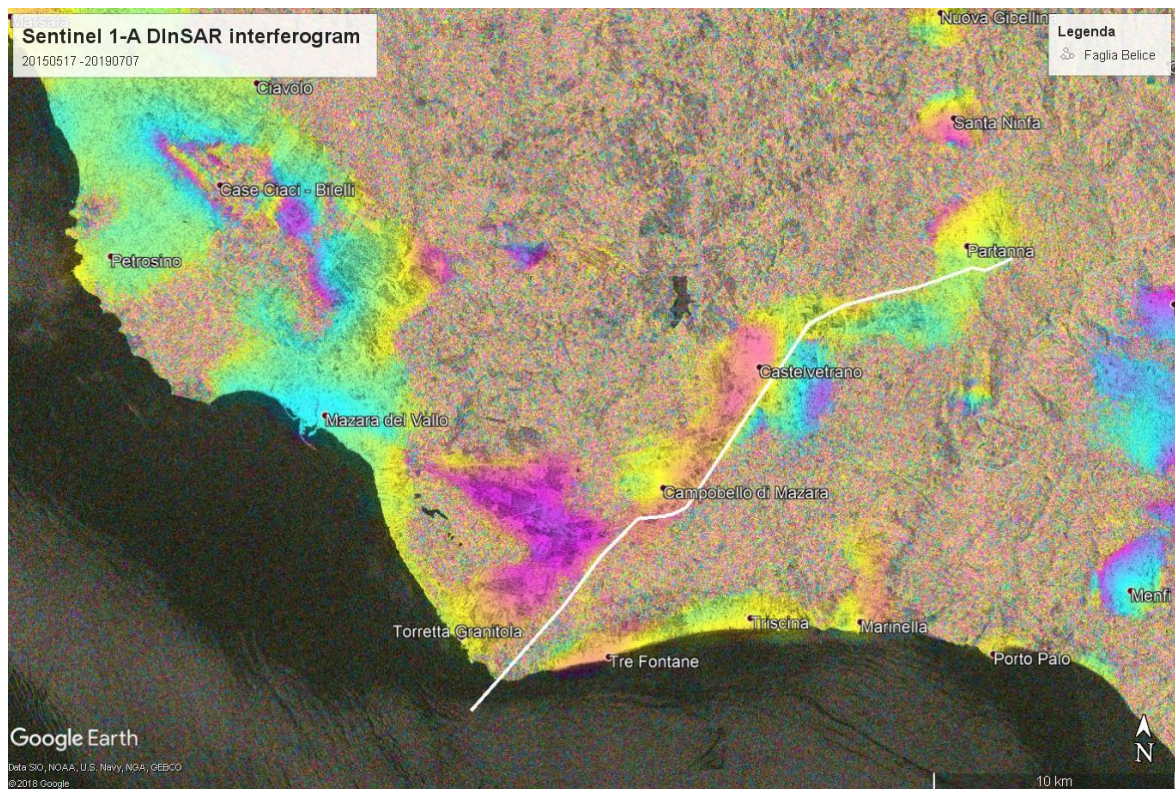
155 **2. Data and methods**

156 *2.1 InSar data*

157 In order to detect the ground deformation in western Sicily, we performed a Differential
158 Interferometry Synthetic Aperture Radar (DInSAR) analysis of C-band Sentinel 1A-B
159 data referring to 2015 May 17 and 2019 July 09. The two Sentinel-1 images were acquired
160 in TopSAR Interferometric Wide (IW) mode (VV polarisation) along the 117 ascending
161 orbit. The Sentinel 1 data were processed by GAMMA software, using a spectral diversity
162 method and a procedure able to co-register the SENTINEL pairs with extremely high
163 precision (< 0.01 pixel). The 4 years time spanning interferogram was produced by
164 applying a two-pass DInSAR processing (using the GAMMA software), and we applied a
165 multilook 5x1 (range and azimuth) in order to maintain the full ground resolution
166 (11x13m) and to remove the topographic phase from interferogram the SRTM V4 Digital
167 Elevation Model (DEM) generated by Shuttle Radar Topography Mission (SRTM) with 3
168 arc-second resolution (about 90 m) was used (Jarvis et al., 2008).

169 Inspection of the DInSAR Line Of Sight (LOS) ground deformation confirmed the
170 displacement rate reported in Barreca et al. (2014), with the evidence of two areas
171 characterized by differential ground motion: (i) the first area trends NW–SE and is located
172 between the towns of Marsala and Mazara del Vallo, probably due to intensive water
173 pumping for agriculture; (ii) the second area with a roughly SSW–NNE orientation,
174 corresponding to Campobello di Mazara–Castelvetrano alignment (CCA), is characterized
175 by about $\frac{1}{4}$ of fringe (7 mm) of differential ground motion.

176



177

178 **Figure 3** Phase DInSAR interferogram of SW Sicily spanning the period 2015 May 17 and 2019 July 09

179

180 *2.2. GNSS data*

181 In 1992 the Italian IGM (Istituto Geografico Militare – www.igmi.org) started the GPS
 182 measuring of a network made up of 1260 benchmarks, about 20 km far from each other
 183 and extended over the whole Italy. We have reoccupied five IGM benchmarks in South-
 184 western Sicily in order to calculate the surface velocity map and to obtain independent
 185 information on strain rate accumulation on the Castelvetrano-Campobello fault revealed by
 186 interferometric data. Every single session of data acquisition span 4–5 h for the first IGM
 187 campaign in 1994 and 5–13 h for the 2013 and 2016 surveys.

188 The novelty of this paper, if compared to Barreca et al., 2014 are: 1) a new dataset (2016)
 189 of GPS data and 2) a largely improved spatial coverage obtained thanks to the eight GNSS
 190 stations managed by University of Palermo (black dots, Fig. 4), spanning the period 2008-

191 2016. Indeed, since 2007, the University of Palermo developed a relevant project to
192 guarantee the presence of several permanent station at Palermo, Trapani, Agrigento and
193 Caltanissetta. After the CORS (Continuous Operating Reference Stations) installation, in
194 the last years, several test have been carried out for technical and scientific purposes,
195 aiming to perform experimental research for GNSS positioning, topographic and
196 cartographic activities and earthquake supporting. In the last few years, many other studies
197 involved the use of UNIPA CORS network, and recently, the results from GNSS have been
198 integrated to remote sensing applications (Dardanelli et al. 2014, Pipitone et al. 2018).



199

200 **Figure 4** Distributed UNIPA CORS network

201

202 The CORS GNSS network for real time and post-processing monitoring managed by the
203 University of Palermo consists of nine CORS far away from each other from 22 to 80
204 kilometres.

205 We processed the GPS data using the GAMIT/GLOBK software (Herring et al., 2018;
206 Herring et al., 2015) with IGS (International GNSS Service) precise ephemerides. We tied

207 the measurements to an external global reference frame by including in our analysis the
208 data from CGPS stations belonging to the IGS and EURA networks, many of which
209 operating since 1994. The loosely constrained daily solutions were then transformed into
210 ITRF2008 (Altamimi et al., 2011) and then rotated to obtain the velocity field into a fixed
211 Europe reference frame. Furthermore, the velocity solutions (Tab.1 and Fig.5) have been
212 used to derive continuous horizontal velocity and strain rate fields in western Sicily. We
213 have applied the method described by Haines and Holt (1993), improved by Holt and
214 Haines (1995) and later used also in other papers (Haines et al., 1998; Kreemer et al.,
215 2000). Besides plates boundary zones (Kreemer et 2000; Beavan and Haines, 2001) this
216 method has been applied also to seismogenic areas both on a regional and local scale
217 (Mattia et al., 2009, 2012; Barreca et al., 2014) and to volcanic areas (Bruno et al., 2012).
218 See Bruno et al. (2012) for more details on the methodology.

Site	Long. (deg)	Lat. (deg)	Ve (mm/yr)	Vn (mm/yr)	Se (mm/yr)	Sn (mm/yr)
AGRG	13.601	37.320	-2.42	2.64	0.92	0.91
ALCM	12.956	37.974	-1.11	3.06	1.23	1.22
BCMA	12.766	37.648	-0.84	2.93	1.57	1.52
CAMP	12.745	37.629	-1.20	2.55	0.91	0.90
FGR2	12.662	37.567	-1.51	2.80	1.47	1.27
MGAI	13.193	37.864	-0.45	3.78	1.54	1.49
MGRA	12.762	37.895	-0.88	2.48	1.55	1.47
PART	13.110	38.040	-1.33	3.96	1.29	1.28
PAUN	13.348	38.106	-1.07	4.70	1.52	1.50
PRIZ	13.437	37.719	-0.90	3.00	1.31	1.28
SEL1	12.836	37.587	-1.73	2.60	1.52	1.50
SETA	14.042	37.486	-0.53	2.05	1.50	1.49
TERM	13.702	37.983	-1.18	3.76	0.97	0.96
TLIP	12.716	37.745	-2.03	2.06	1.47	1.45
TRAP	12.541	38.013	-0.86	2.54	1.48	1.45

219 **Table 1.** Site code, geodetic coordinates, East and North velocity components and associated errors for all
220 benchmarks.

221

222 **3. Results**

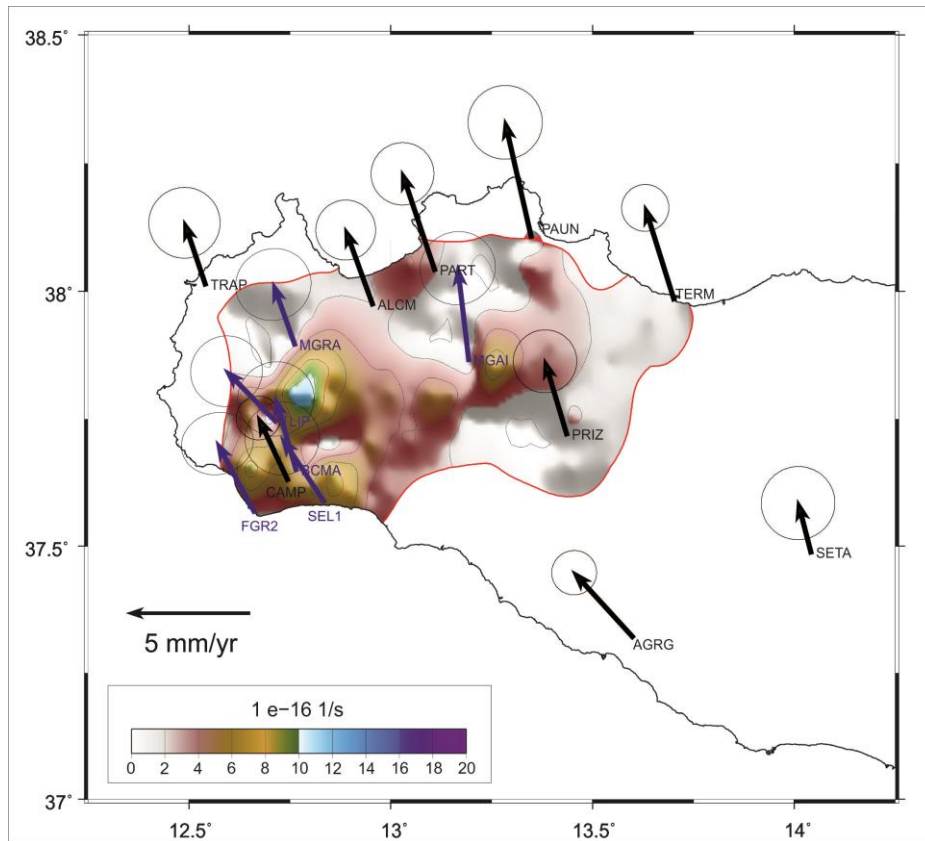
223 The Sentinel 1A-B DInSAR data confirmed the displacement rate reported in Barreca et al.
224 (2014), evidencing a differential LOS displacements rate of about 2 mm/year along the
225 roughly SSW–NNE Campobello di Mazara–Castelvetrano alignment (CCA).

226 The horizontal velocity field in the Eurasian fixed reference frame shows that the GNSS
227 stations of western Sicily move with velocities ranging from about 2.1 to 4.8 mm/yr along
228 NNW to NW directions. The magnitude of the horizontal velocities decreases from almost
229 5 mm/yr along the Northern coastline to the mean value of 2.9 mm/yr along the most
230 western sector of the investigated area and along the CCA alignment. Furthermore, the
231 velocity values slightly decrease across the CCA alignment, from East to West, from about
232 3.2 mm/yr (SEL1) to values of 2.8 mm/yr (CAMP). The decrease in magnitude of velocity
233 is accompanied by minor azimuth variations. The different velocities affecting the stations
234 lying on the different sides of the CCA alignment, although small, are in agreement with
235 the field evidences of active deformation found by Barreca et al. (2014).

236 We have also inverted the GNSS velocities to obtain the shear strain rate distribution. The
237 regions with higher strain concentration are often locations of seismogenic faults and more
238 prone to be the source of future earthquakes, releasing elastic energy accumulated in the
239 neighbourhood over the interseismic time period. Fig. 5 shows that the shear strain rate in
240 western Sicily is mainly distributed along a SW-NE direction that corresponds to the area
241 of the CCA alignment. It reaches maximum values of about $12 \cdot 10^{-16}$ 1/s. Geodetically
242 observed strain rate has some limitations due to the fact that it includes both elastic and
243 anelastic strains, and in many cases it is difficult to differentiate the two components
244 without a priori knowledge. Because only the elastic strain is responsible for earthquakes,
245 try to understand where seismic energy could be released, using geodetic strain, alone is
246 not an exhaustive approach, particularly across faults that are creeping or in regions where
247 significant amounts of deformation take place plastically. Although geological

248 observations have indicated that stress along the CCA alignment is at present released as
249 aseismic creep (Barreca et al., 2014), coseismic ruptures could propagate up to the earth
250 surface, as probably occurred in the past (Barreca et al., 2014), considering that the area is
251 spatially coincident with the macroseismic zone of the 1968 Belice earthquake.

252



253

254 **Figure 5.** Horizontal GNSS velocities with 95% confidence ellipses in the Eurasian reference frame for the
255 measured IGM benchmarks (1994-2016) (blue arrows) and permanent GNSS stations (black arrows) in
256 western Sicily. The magnitude of geodetic shear strain rate is reported as colour map, enclosed by the red
257 line, that indicate 50% resolution level of the map (Kreemer et al., 2000).

258

259 **5. Conclusions**

260 According to measured GPS benchmarks, western Sicily move with velocities ranging
261 from about 2.1 to 4.8 mm/yr along NNW to NW directions, suggesting an intraplate

262 differential geodetic velocity of about 3 mm/yr. Strain rate derived map, decrease of
263 velocity values, and ground deformation rates from the interferometric methods clearly
264 indicate that most of strain is accumulating in SW Sicily and particularly along the CCA
265 alignment, where archaeological remains were displaced by a reverse fault (see Barreca et
266 al., 2014). Maximum of strain rate (see Fig. 5) and differential ground motion (Fig. 4)
267 depict in fact an NNE-SSW trending boundary that well match with the previously mapped
268 CCA tectonic alignment. Here, SAR and GPS methods allowed to define clearly the
269 deformation rate components with vertical and horizontal displacements of 2 mm/yr
270 and 0.5 mm/yr respectively. According to the tectonic setting of the area (see section 2.1),
271 these components are compatible with a high-angle thrust fault displacing, as expected,
272 mainly along the vertical component rather than the horizontal one. New data permit thus
273 to refine better the previously performed geodetic and satellite measurements (see Barreca
274 et al., 2014) and to evaluate the short-term (last five years) deformation rate in the Belice
275 area. Obtained values indicate that the rate of deformation has remained constant during
276 the analysed time span and confirms the low rate of horizontal deformation in the analysed
277 sector, which seems also to suggest a long recurrence time for large earthquakes. Since no
278 significant earthquakes have occurred after the Belice 1968 event, measured deformations
279 seem to suggest that most of stress could be dissipated via aseismic creeping mainly along
280 the CCA alignment. This could be due to a possible diffraction into discrete splays of
281 major deep-seated thrust contacts at shallow crustal level. Splays mainly propagate
282 aseismically within the clayey lithologies characterizing the upper level of the duplex
283 system (see section 2.1). Alternatively, considering the rigidity of carbonates forming the
284 main deep-seated tectonic blocks, the measured strain and the aseismic behaviour of CCA
285 in the last 50 yr (see Barreca et al., 2014) could be interpreted as the (short) non-elastic
286 stage of deformation preceding rupture in the area.

287 To conclude, the combined technique here proposed, when accompanied by field studies,
288 revealed a powerful tool in seismotectonic analysis since it allows monitoring and
289 detecting of active faults even in slowly deforming area such as the one here analysed.

290

291 **Acknowledgments**

292 **The authors thank the referees and the editor for their useful suggestions. We also**
293 **thank all the people involved in field activities and the technicians involved in the**
294 **management of GNSS permanent stations.**

295 **Copernicus Sentinel-1A/B data [2015-2019] are available at the Copernicus Open**
296 **Access Hub (<https://scihub.copernicus.eu>)**

297

298 **References**

299 - Altamimi, Z, X. Collilieux and L. Metivier (2011). ITRF2008: an improved solution of
300 the International Terrestrial Reference Frame, *J. Geod.*, 85(8):457–473,
301 doi:10.1007/s00190-011-0444-4.

302 - Anderson, H, and J. Jackson (1987). Active tectonics of the Adriatic Region. *Geophys.*
303 *J.R. Astr. Soc.*, 91, 937-983.

304 - Avellone, G, M.R. Barchi, R. Catalano, M.G. Morticelli and A. Sulli (2010). Interference
305 between shallow and deep-seated structures in the Sicilian fold and thrust belt, Italy.
306 *Journal of the Geological Society* 167, 109–126, doi:10.1144/0016-76492008-163.

307 - Barreca, G, and F.E. Maesano (2012). Restraining stepover deformation superimposed on
308 a previous fold-and thrust-belt: A case study from the Mt. Kumeta–Rocca Busambra ridges
309 (western Sicily, Italy). *Journal of Geodynamics*. doi: 10.1016/j.jog.2011.10.007

- 310 - Barreca, G, F.E Maesano and S. Carbone (2010). Tectonic evolution of the Northern
311 Sicilian-Southern Palermo Mountains range in Western Sicily: insight on the exhumation
312 of the thrust-involved foreland domains. *It. J. Geosci. (Boll. Soc. Geol. It.)*, 129 (3), 234-
313 247
- 314 - Barreca, G., V. Bruno, C. Cocorullo, F. Cultrera, L. Ferranti, F. Guglielmino, L.
315 Guzzetta, M. Mattia, C. Monaco and F. Pepe (2014). Geodetic and geological evidence of
316 active tectonics in south-western Sicily (Italy), *J. Geod.*, 82:138–149, doi:
317 10.1016/j.jog.2014.03.004.
- 318 - Beavan, J. and J. Haines (2001). Contemporary horizontal velocity and strain rate fields
319 of the Pacific-Australian plate boundary zone through New Zealand, *J. Geophys. Res.*, 106,
320 741–770, doi:10.1029/2000JB900302.
- 321 - Bello, M, A. Franchino, and S. Merlini (2000). Structural model of eastern Sicily.
322 *Memorie della Società Geologica Italiana* 55, 61–70.
- 323 - Ben-Avraham, Z, M. Boccaletti, G. Cello, M. Grasso, F. Lentini, L. Torelli and L.
324 Tortorici (1990). Principali domini strutturali originatisi dalla collisione neogenico-
325 quaternaria nel Mediterraneo centrale: *Memorie della Società Geologica Italiana*, v. 45, p.
326 453–462.
- 327 - Bosi, C, R. Cavallo and V. Francaviglia (1973). Aspetti geologici e geologico-tecnici del
328 terremoto della Valle del Belice del 1968. *Mem. Soc. Geol. It.*, 12, 81-130.
- 329 - Bottari, A. (1973). Attività sismica e neotettonica della Valle del Belice. *Ann. Geof.*,
330 XXVI (1), 55-83.
- 331 - Bottari, C, S.C. Stiros and A. Teramo (2009). Archaeological evidence for
332 destructive earthquakes in Sicily between 400 B.C. and A.D. 600. *Geoarchaeology* 24
333 (2),147–175, <http://dx.doi.org/10.1002/gea.20260>.

334 - Bruno, V., M. Mattia, M. Aloisi, M. Palano, F. Cannavò and W. E. Holt (2012). Ground
335 deformations and volcanic processes as imaged by CGPS data at Mt. Etna (Italy) between
336 2003 and 2008, *J. Geophys. Res.*, 117, B07208, doi:10.1029/2011JB009114.

337 - Catalano, R, B. D'Argenio and L. Torelli (1989). A geological section from Sardinia
338 Channel to Sicily Straits based on seismic and field data. In: Boriani, A.B., Piccardo, M.,
339 Vai, G.B (Eds.), *The lithosphere in Italy: Advances in Earth Science Research. Atti dei*
340 *Convegni Lincei*, vol. 80. Italian National Committee for the International Lithosphere
341 Program, pp. 110–128.

342 - Catalano, R, A. Franchino, S. Merlini and A. Sulli (2000). Central western Sicily
343 structural setting interpreted from seismic reflection profiles. *Memorie della Società*
344 *Geologica Italiana* 55, 5–16.

345 - Dardanelli, G., G. La Loggia, N. Perfetti, F. Capodici, L. Puccio and A. Maltese (2014).
346 Monitoring displacements of an earthen dam using GNSS and remote sensing, in Proc.
347 SPIE 9239, *Remote Sensing for Agriculture, Ecosystems, and Hydrology XVI*,
348 Amsterdam, Netherlands, 923928.

349 - De Panfilis, M, and L. Marcelli (1968). Il periodo sismico della Sicilia occidentale
350 iniziato il 14 gennaio 1968. *Ann. Geof.*, XXI, 4, 343-420.

351 - Devoti, R, A. Esposito, G. Pietrantonio, A.R. Pisani and F. Riguzzi (2011). Evidence of
352 large scale deformation patterns from GPS data in the Italian subduction boundary, *Earth*
353 *Planet. Sci. Lett.*, 311, 230-241, doi: 10.1016/j.epsl.2011.09.034.

354 - Dewey, J.F, M.L Helman, E. Turco, D.H.W, Hutton and S.D Knott (1989). Kinematics of
355 the Western Mediterranean, in Coward, M.P., Dietrich, D.,and Park, R.G., eds., *Alpine*
356 *Tectonics: Geological Society of London Special Publication* 45, p. 265–283.

357 DISS Working Group, 2010. <http://diss.rm.ingv.it/diss/>, © INGV 2010.

358 - Ferranti, L, J.S Oldow, B. D'Argenio, R. Catalano, D. Lewis, E. Marsella, G. Avellone,
359 L. Maschio, G. Pappone, F. Pepe and A. Sulli (2008). Active deformation in Southern Italy,
360 Sicily and southern Sardinia from GPS velocities of the Peri-Tyrrhenian Geodetic Array
361 (PTGA). *Ital. J. Geosci.* 127 (2), 299–316.

362 - Finetti, I.R., Lentini, F., Carbone, S., Del Ben, A., Di Stefano, A., Forlin, E., Guarnieri,
363 P., Pipan, M., Prizzon, A., (2005) Geological outline of Sicily and Lithospheric Tecton-
364 odynamics of its Tyrrhenian Margin from new CROP seismic data. In: Finetti, I.R.(Ed.),
365 CROP PROJECT: Deep Seismic Exploration of the Central Mediterranean and Italy.
366 Elsevier, Amsterdam.

367 - Guidoboni, E, A. Comastri and G. Traina (1994). Catalogue of Ancient Earthquakes in
368 the Mediterranean Area up to the 10th Century: Bologna, ING, 504 p.

369 - Guidoboni, E, A. Muggia, C. Marconi and E. Boschi (2002). A case study in archaeo-
370 seismology. The collapses of the Selinunte Temples (Southwestern Sicily): two earthquakes
371 identified. *Bull. Seismol. Soc. Am.* 92, 2961–2982.

372 - Haas, J.E, and R.S. Ayre (1969). The western Sicily earthquake of 1968. National
373 Academy of Engineering Report, National Academy of Science. P.70.

374 - Haines, A. J., A. Jackson, W. E. Holt and D. C. Agnew (1998). Representing distributed
375 deformation by continuous velocity fields, *Sci. Rep.* 98/5, Inst. of Geol. and Nucl. Sci.,
376 Lower Hutt, N. Z.

377 - Haines, A. J. and W. E. Holt (1993). A procedure for obtaining the complete horizontal
378 motions within zones of distributed deformation from the inversion of strain rate data, *J.*
379 *Geophys. Res.*, 98, 12,057–12,082, doi:10.1029/93JB00892.

380 - Herring, T. A., R. W. King, M. A. Floyd, S. C. McClusky (2015), GAMIT Reference
381 Manual. GPS Analysis at MIT, Mass. Inst. of Technol., Cambridge.

382 - Herring, T. A., M. A. Floyd, R. W. King, S. C. McClusky (2015), GLOBK Reference
383 Manual. Global Kalman filter VLBI and GPS analysis program, Mass. Inst. of Technol.,
384 Cambridge.

385 - Jarvis, A., H.I. Reuter, A. Nelson and E. Guevara (2008), Hole-filled SRTM for the globe
386 version 4, available from the CGIAR-CSI SRTM 90m Database. (Available at
387 <http://srtm.csi.cgiar.org>).

388 - Holt, W. E. and A. J. Haines (1995). The kinematics of northern South Islands, New
389 Zealand, determined from geologic strain rates, *J. Geophys. Res.*, 100, 17,991–18,010,
390 doi:10.1029/95JB01059. Jarvis et al., 2008

391 - Kreemer, C., W. E. Holt, S. Goes and R. Govers (2000). Active deformation in eastern
392 Indonesia and the Philippines from GPS and seismicity data, *J. Geophys. Res.*, 105(B1),
393 663–680, doi:10.1029/1999JB900356.

394

395 - Lavecchia, G, F. Ferrarini, R. de Nardis, F. Visini and S. Barbano (2007). Active
396 thrusting as a possible seismogenic source in Sicily (Southern Italy): some insights from
397 integrated structural-kinematic and seismological data, *Tectonophysics*, 445, 145–167.

398 - Marcelli, L, and G. Pannocchia (1971). Uno studio analitico sui dati ipocentrali di 10
399 terremoti avvenuti in Sicilia occidentale nel gennaio del 1968. *Ann. Geofis*, 24, 287-306.

400 - Mattia, M., M. Palano, V. Bruno, F. Cannavò (2009). Crustal motion along the Calabro-
401 Peloritano Arc as imaged by twelve years of measurements on a dense GPS network,
402 *Tectonophysics*, 476, 528–537.

403 - Mattia, M., V. Bruno, F. Cannavò, M. Palano (2012). Evidences of a contractional pattern
404 along the northern rim of the Hyblean Plateau (Sicily, Italy) from GPS data, *Geol. Acta*,
405 vol. 10, n. 12, 63-70.

406 - Michetti, A. M, F. Brunamonte and L. Serva (1995). Paleoseismological Evidence in the
407 Epicentral Area of the January 1968 Earthquakes, Belice, Southwestern Sicily. in: L. Serva
408 and D. B. Slemmons (eds): "Perspectives in Paleoseismology", A.E.G. Special Publication,
409 6, 127-139.

410 - Monaco, C, S. Mazzoli and L. Tortorici (1996). Active thrust tectonics in western Sicily
411 (southern Italy): the 1968 Belice earthquakes sequence. Terra Nova, 8, 372-381.

412 - Palano, M., L. Ferranti, C. Monaco, M. Mattia, M. Aloisi, V. Bruno, F. Cannavò and G.
413 Siligato (2012). GPS velocity and strain fields in Sicily and southern Calabria, Italy:
414 updated geodetic constraints on tectonic block interaction in the central Mediterranean. J.
415 Geophys. Res., 117, B07401.

416 - Pipitone, C., A. Maltese, G. Dardanelli, M. Lo Brutto and G. La Loggia (2018).
417 Monitoring water surface and level of a reservoir using different remote sensing
418 approaches and comparison with dam displacements evaluated via GNSS, Remote Sens.,
419 10, 71.

420 - Pondrelli, S, S. Salimbeni, G. Ekström, A. Morelli, P. Gasperini and G. Vannucci (2006).
421 The Italian CMT dataset from 1977 to the present, Phys. Earth Planet. In., 159, 286-303,
422 doi: 10.1016/j.pepi.2006.07.008.

423 - Rigano, R, B. Antichi, L. Arena, R. Azzaro and M.S. Barbano (1999). Sismicità e
424 zonazione sismogenetica in Sicilia occidentale. GNGTS, 1998

425 - Rovida, A, R. Camassi, P. Gasperini and M. Stucchi (2011). CPTI11, The 2011 Version
426 of the Parametric Catalogue of Italian Earthquakes, Milano,
427 Bologna.<http://emidius.mi.ingv.it/CPTI>

428

429